Determination of optimum cooling conditions for continuous casting by a meshless method

A Khosravifard, MR Hematiyan and L Marin

Proceedings of the Institution of Mechanical Engineers, Part C: Journal of Mechanical Engineering Science published online 15 August 2012
DOI: 10.1177/0954406212457325

Original Article

Institution of MECHANICAL ENGINEERS
Journal of MECHANICAL ENGINEERING SCIENCE

Proc IMechE Part C:
J Mechanical Engineering Science
0(0) 1–14

DOI: 10.1177/0954406212457325
pic.sagepub.com
SAGE

Determination of optimum cooling conditions for continuous casting by a meshless method

A Khosravifard[1], MR Hematiyan[1] and L Marin[2,3]

Abstract

An inverse technique based methodology for the optimal control of the solidification front motion in the continuous casting of pure metals with temperature-dependent material properties is proposed. In this method, to achieve specific mechanical and metallurgical properties of the final product, a predefined motion of the solidification front is selected. A history of the heat flux on the fixed boundaries of the problem is then computed, which would result in an actual motion of the solidification front representing the best match for the desired one. A sensitivity analysis of the inverse problem is efficiently carried out by a truly meshless method. The proposed inverse technique is applied for the design of the continuous casting of pure metals with temperature-dependent thermo-physical properties. The efficiency of the proposed method is demonstrated through some numerical examples.

Keywords

Continuous casting, inverse method, meshless method, pseudo-heat source method

Date received: 1 May 2012; accepted: 17 July 2012

Introduction

The continuous casting process is a means of production of high-quality metals and alloys in a cost-efficient manner. The continuous casting process allows for low-cost production of metal ingots because of the inherently lower costs of continuous production. If judiciously designed, the process also provides great control over the quality of final products. Considerable increase in yield, generation of uniform products, energy efficiency, and higher manpower productivity are the main advantages of continuous casting.[1] The continuous casting process is most commonly used for the production of steel, as well as aluminum and copper.

When dealing with the numerical modeling of the continuous casting process, there are two distinct classes of problems. In the first class, the governing equation of solidification is solved directly based on the known initial and boundary conditions. The aim of this type of problem is to obtain the temperature distribution in the solidifying part during the process, as well as the time-dependent location of the solid–liquid interface. Such problems are known as direct solidification problems. In the second class, either the location of the solidifying front or the cooling conditions are sought based on temperature measurements,[2,3] or an optimum boundary cooling condition is sought for obtaining a prescribed motion of the solidification front.[4] These problems are known as inverse solidification problems.

Since the governing equation of solidification is non-linear, for most practical situations, it is difficult or even impossible to obtain closed-form analytical solutions. Consequently, computational methods have been widely used for the analysis of direct as well as inverse casting problems. Weckman and Niessen[5] utilized the finite element method (FEM) to solve the steady-state thermal problem associated with the continuous casting of A6063 aluminum cylindrical ingots. Their method allows for the calculation of effective heat transfer coefficients on the boundaries of the ingot. In order to obtain the temperature distribution in the strand, based on the known boundary conditions on the strand surface in a continuous casting process, Laitinen and Neittaanmäki[6] used the enthalpy formulation along with the FEM. Modeling of the heat flow in the continuous casting process by the finite difference method (FDM) has been

[1]Department of Mechanical Engineering, Shiraz University, Shiraz, Iran
[2]Institute of Solid Mechanics, Romanian Academy, Bucharest, Romania
[3]Centre for Continuum Mechanics, Faculty of Mathematics and Computer Science, University of Bucharest, Bucharest, Romania

Corresponding author:
MR Hematiyan, Department of Mechanical Engineering, Shiraz University, Shiraz, Iran.
Email: mo.hematiyan@gmail.com, mhemat@shirazu.ac.ir

performed by Lally et al.[7] Their model includes non-linear thermodynamic and transport properties of the medium. Theodorakakos and Bergeles[8] solved the steady-state Navier–Stokes equations by the FDM to model the flow of steel in a continuous casting process. Their method was aimed at the understanding of the free wave and the interface surface wave behavior of the flow. Fic et al.[9] used the boundary element method (BEM) for the analysis of the phase change heat transfer in the strand during continuous casting. Their method is applicable to the continuous casting of pure materials since it is assumed that the phase change is isothermal.

Ha et al.[10] conducted a numerical simulation study on the molten steel in a continuous casting process in the presence of electromagnetic fields. By solving the three-dimensional (3D) mass, momentum, and energy conservation equations, along with Maxwell's equations for the electromagnetic field coupled with a flow field, they investigated the effect of the magnetic field on the turbulent flow field, heat transfer, and solidification phenomena. Risso et al.[11] evaluated the thermal stresses and plastic strains in the solid shell at the initial stage of a steel continuous casting process.

Recently, mesh-free methods have also been used successfully for the analysis of heat transfer[12,13] and solidification problems.[14] Being independent of a predefined mesh of elements, mesh-free methods are well suited for the analysis of moving boundary[14] and large deformation problems.[15] Zhang et al.[14] applied the finite point method (FPM) to model metal solidification process in continuous casting, at the same time using the enthalpy method to account for the latent heat effects. Zhang et al.[16] simulated the solidification process and the thermal stress of continuous casting billet in mold by an integrated thermo-mechanical meshless analysis. They used the FPM for the thermal part of the simulation and the meshless local Petrov–Galerkin method for the elastic–plastic part. Ko et al.[17] established a 3D numerical model for the analysis of the thermal behavior of copper molds in the continuous casting process.

Numerical methods have also been used for the inverse analysis of the continuous casting process. Based on a non-linear constrained optimization technique, Engl and Langthaler[18] computed the values of the external cooling and also the casting speed to obtain a desirable solidification front. Binder et al.[19] used temperature measurements during the secondary cooling of steel in continuous slab casting for determination of the solidification front position. They also determined a cooling strategy that leads to a prescribed solidification front. Hill and Wu[20] also used inverse techniques for the determination of the solidification front in the continuous casting of steel. They used integral formulations to establish a so-called normalized pseudo-steady-state temperature as an upper bound to the normalized actual temperature. By this approach, an upper bound for the solidification front position was obtained. Grever et al.[21] determined a cooling strategy for the continuous casting process which insures that the final solidification takes place within the 'soft-reduction' zone and reformulated the problem of finding an appropriate cooling strategy as a finite-dimensional non-linear optimization problem. Nowak et al.[22] used temperature measurements in the solid phase and sensitivity coefficients for the prediction of the interface location in the continuous casting process and formulated the problem as an inverse geometrical thermal problem using the BEM. Cheung and Garcia[23] used an artificial intelligence heuristic search method along with a numerical heat transfer model to find optimized cooling conditions, which results in defect-free billet production with a minimum metallurgical length.

Later, Nowak et al.[24] used the Bezier curves to model the interface between the solid and liquid phases and formulated a geometrical inverse problem for the identification of the phase change front in continuous casting. In this study, the influence of the measurement errors on the accuracy of the phase change front location was determined. Santos et al.[25] developed a computational algorithm aimed at controlling the quality of steel billets produced by continuous casting using a genetic search algorithm and a knowledge base of operational parameters for selection of a set of cooling conditions in order to attain highest product quality. A 3D numerical solution of the inverse boundary problem for the continuous casting of alloys was presented by Nowak et al.[26] The objective of their work was to estimate the heat fluxes on the external boundaries of the ingot based on temperature measurements. Slota[27] solved an inverse Stefan problem for the reconstruction of the function describing the boundary conditions along the primary and secondary cooling zones in the 2D and 3D continuous casting of pure metals. In the numerical calculations, the Tikhonov regularization method and a genetic algorithm were used. Nowak et al.[2] have presented a numerical solution for the inverse boundary problem in a continuous casting of an aluminum alloy. Recently, Slota[3] proposed a method for the retrieval of heat fluxes and heat transfer coefficient in the continuous casting of pure metals based on temperature measurements. Fazeli and Mirzaei[28] have conducted a comparative survey on the methods used for the identification of the solid–liquid interface in a cold storage system. By measuring the temperature on the outer surface of the storage, the shape of the interface was estimated in Fazeli and Mirzaei.[28]

The inverse solidification problem that is dealt with in this study is considered as a design problem. It should be mentioned that, in some inverse solidification problems, the objective is to retrieve the existing cooling conditions or the solidification front position based on temperature measurements. However, the objective of some other inverse problems, which are

considered as design problems, is to calculate an optimum history of the heat flux distribution on the boundaries of the problem to achieve a predefined morphology of the solidification front.

The inverse approach used in this article for obtaining an optimum heat flux history is based on the so-called pseudo-heat source method. In this approach, for modeling the solidification process, the governing equations of heat conduction are utilized. However, in order to account for the liberation of latent heat, an imaginary heat source near the solidification front is considered. Consideration of the pseudo-heat source in this method is the key difference of this approach with respect to those used by other researchers. Using this approach, the inverse problem can be tackled much easier and more efficiently.[29] This article is a continuation of the previous study of the authors[4] with an emphasis on the applicability of the design process. The key contribution of this study is that the temperature dependence of the casting thermo-physical properties is taken into account. Also, the design of an important production process is considered in detail. Several various situations for the continuous casting of iron are investigated through numerical examples, while very good results are obtained. In both the previous papers that utilize the pseudo-heat source method, i.e. Khosravifard and Hematiyan[4] and Hematiyan and Karami,[29] although acceptable results were obtained, the thermo-physical properties of the medium are considered to be temperature independent. In this article, all thermo-physical properties of the medium are considered temperature dependent, which makes the inverse problem much more difficult. This broadens the area of applicability of the proposed method. It should be emphasized that taking into account the temperature dependence of the material properties imposes a great non-linearity on the inverse problem and new strategies should be utilized for obtaining a stable solution. Such strategies are further discussed in detail herein.

Various numerical methods can be used for the sensitivity analysis of the problem. As mentioned previously, the FEM and BEM have been used for this purpose. However, utilization of the meshless methods for the sensitivity analysis of non-linear problems can be beneficial. Meshless methods were introduced in the mid 1990s and are still being an active research area in engineering and sciences.[30–32] It is known that the modeling of temperature-dependent material properties using the BEM is cumbersome. The FEM faces some difficulties when modeling abrupt changes in the material properties, which occur on the sides of the solidification front. However, mesh-free methods can easily deal with temperature-dependent material properties. Additionally, due to their good interpolation characteristics, modeling abrupt changes in the material properties can be performed with acceptable accuracy. The sensitivity analysis of the inverse method proposed in this article is performed by a truly meshless method, i.e. the meshless improved radial point interpolation method or simply the IRPIM.[13] In this method, the Cartesian transformation method (CTM) is used for the meshless evaluation of domain integrals. The meshless IRPIM is a suitable tool for the analysis of non-linear transient problems.[13] Since the sensitivity analysis used in this article is based on the solution of several non-linear transient problems, the IRPIM is an appropriate tool for this purpose.

Mathematical model of the continuous casting process

Figure 1 is a schematic representation of the continuous casting process. The process consists of several stages. In the first stage, the liquid metal is poured into a chilled mold and a thin solid shell is produced. In the next stage, the metal is further cooled by a direct spray of water and the thickness of the solidified shell is increased. Finally, the solidified metal is flame cut and cooled to room temperature.

Continuous casting: The direct problem

The objective of a direct continuous casting problem is determination of the temperature distribution in the metal during the process, as well as the time-dependent location of the solidification front. Figure 2 depicts the problem geometry and boundary conditions associated with a typical continuous casting process. Due to the symmetry of the problem, only a quarter of the problem domain is required to be modeled. The mathematical model of the continuous casting process is governed by the general heat conduction equation with an internal heat generation source to account for the liberation of latent heat[25]

$$\rho(T)c(T)\frac{\partial T}{\partial t} = \nabla(k(T)\nabla T) + g(\mathbf{x}) \tag{1}$$

where ρ is the mass density, c the specific heat, k the thermal conductivity, T the temperature, and g the heat generation source per unit volume. The initial and boundary conditions for equation (1) associated with a continuous casting process are as follows:

$$\begin{aligned} &T(\mathbf{x},0) = T_i, && \text{in the problem domain}\\ &q(\mathbf{x},t) = \bar{q}_j(\mathbf{x},t), && j = 1, 2\\ &q(\mathbf{x},t) = 0, && \text{on the insulated boundaries} \end{aligned}$$

Continuous casting: The inverse problem

The objective of the inverse continuous casting process followed in this article is the determination of a

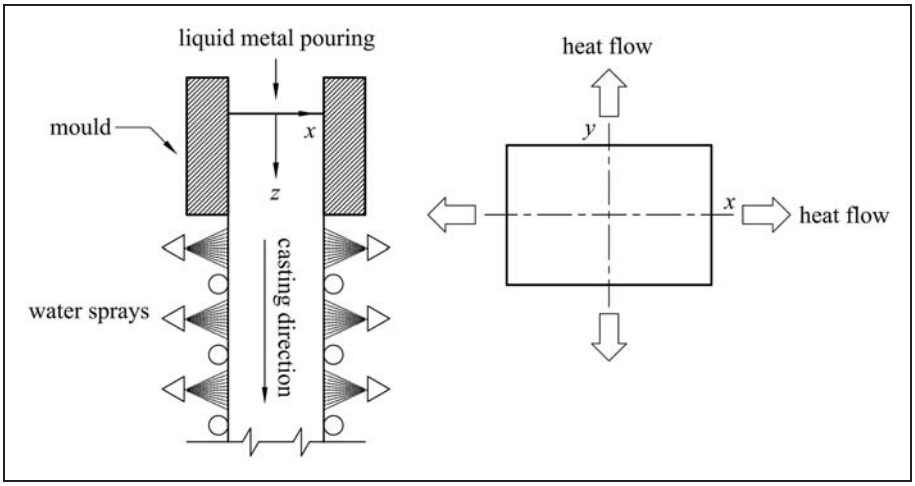

Figure 1. Schematic representation of the continuous casting process.

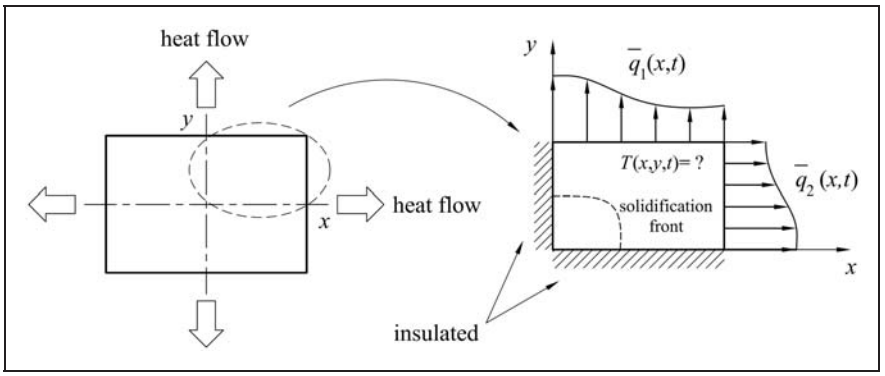

Figure 2. Model of a typical continuous casting process.

heat flux history that would result in a predefined motion of the solidification front. More specifically, the time-dependent position of the solidification front is selected based on a desired motion path and velocity of the front. Then, an optimization problem is defined in which the objective function is the temperature difference between the actual and the desired problems at the predefined position of the solidification front. The unknown heat fluxes on the boundaries of the problem are independent variables of the objective function. The minimization of the objective function gives specific heat fluxes that lead to a motion of the solidification front which is as close as possible to the desired motion.

Problem statement and formulation. A domain which is initially occupied by a liquid metal at $T \geqslant T_m$ is considered, where T_m is the melting point of the metal (Figure 3). At time $t = 0$, a part of the domain boundary is cooled, causing the initiation of the solidification process. This part of the boundary is denoted by Γ_q, while the remaining boundary, on which prescribed boundary conditions are applied, is denoted by Γ_p. As the solidification process starts, a moving boundary $\Gamma_I(t)$ is formed, which separates the solidified part of the domain Ω_s from the liquid part Ω_l. We assume that the desired position of the moving boundary, i.e. the solidification front, is predefined at $(N+1)$ discrete instances of time t_i, $i = 0, 1, \ldots, N$. To this end, the value of the heat flux at N_q points on the boundary Γ_q should be evaluated. This is

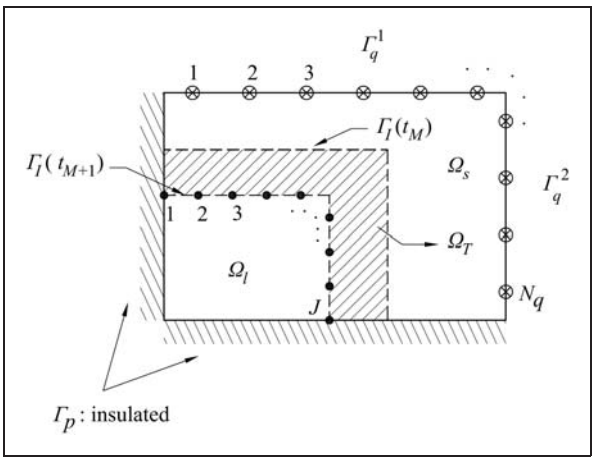

Figure 3. Terminology of the inverse continuous casting process.

accomplished by minimizing the temperature difference between J sampling points on the moving boundary and the desired temperature, i.e. T_m.

To obtain the numerical formulation of the inverse problem, we suppose that M steps of the problem analysis are performed, i.e. the heat fluxes and the temperature distribution within the domain at time instances t_i, $i = 0, 1, \ldots, M$ are evaluated. Now, the values of the heat fluxes at N_q points on the boundary $\Gamma_q = \Gamma_q^1 + \Gamma_q^2$ are sought. These values cause the moving boundary to advance from its position at time $t = t_M$ to a new position at $t = t_{M+1}$, i.e. $\Gamma_I(t_{M+1})$. That part of the domain which is solidified during one time step of the problem is termed as the transition zone and is denoted by Ω_T. It should be highlighted that the transition zone is not a physical domain that exists in the casting. This zone represents the amount of matter that is solidified during each time step of the analysis of the problem. In fact, this zone is a predefined design factor. For computational purposes, a vector $\mathbf{q}_B$ is defined, which contains the values of the heat fluxes to be evaluated, namely

$$\mathbf{q}_B = \lfloor\, q_1 \quad q_2 \quad q_3 \quad \cdots \quad q_{N_q} \,\rfloor^{\mathrm{T}} \tag{2}$$

To account for the effects of the latent heat, a pseudo-heat source is placed in the transition zone. At each time step of the analysis, it is assumed that the heat source is uniformly distributed in the transition zone. The role of this heat source is to provide as much heat to the domain as it is released when the amount of the material contained in Ω_T is solidified. The intensity of this heat source per time per unit volume is obtained as

$$g = \frac{mL}{V\Delta t} = \frac{\rho L}{\Delta t} \tag{3}$$

where m and V are the mass and volume of the material contained in the transition zone, respectively, L the latent heat of solidification, ρ the mass density and $\Delta t = t_{M+1} - t_M$.

Based on an initial guess for the vector $\mathbf{q}_B$ and the temperature distribution at time $t = t_M$ as initial condition, the values of the temperature at J sampling points at time $t = t_{M+1}$ are calculated. The calculated values of the temperature at these sampling points are collected in a vector denoted by $\mathbf{T}$. Since we wish the location of the sampling points and that of the solidification front to coincide, the temperature at the sampling points should be as close as possible to the melting temperature of the metal. To achieve this goal mathematically, a vector $\mathbf{Y}$, whose values are equal to T_m, is formed. Consequently, one obtains an objective function defined as the norm of the vector given by the difference between $\mathbf{T}$ and $\mathbf{Y}$. The design variables of this objective function are the unknown heat fluxes on the boundary. Since the main difficulty with all types of inverse problems is their ill-posedness, the number of measurements should be greater than the number of unknown design variables, that is $J > N_q$. In this way, the problem becomes over-determined and the chances to find a physically meaningful solution increase. However, the results may be oscillatory and usually the addition of a regularization term to the objective function is necessary to improve the stability of the inverse algorithm. Consequently, the objective function is defined as

$$S = \big(\mathbf{Y} - \mathbf{T}(\mathbf{q}_B)\big)^{\mathrm{T}}\big(\mathbf{Y} - \mathbf{T}(\mathbf{q}_B)\big) + \alpha \mathbf{q}_B^T \mathbf{q}_B \tag{4}$$

where α is the regularization parameter. The method used for the definition of the objective function in this study is most commonly known as the Tikhonov regularization method. The vectors $\mathbf{Y}$ and $\mathbf{T}$ in equation (4) contain the desired and estimated values of the temperature at the sampling points, respectively, i.e.

$$\mathbf{Y} = \begin{Bmatrix} T_m \\ T_m \\ T_m \\ \vdots \\ T_m \end{Bmatrix}_{J\times 1}, \quad \mathbf{T} = \begin{Bmatrix} T_1 \\ T_2 \\ T_3 \\ \vdots \\ T_J \end{Bmatrix} \tag{5}$$

The first term on the right-hand side of equation (4) guarantees a solution that results in the minimum difference between the estimated and desired temperatures at the sampling points, while the second term damps the oscillations of the elements of the vector $\mathbf{q}_B$. The vector of heat fluxes that minimizes the objective function is obtained by minimizing the functional (4), i.e.

$$\frac{\partial S}{\partial \mathbf{q}_B} = -2\mathbf{X}\big(\mathbf{Y} - \mathbf{T}(\mathbf{q}_B)\big) + 2\alpha \mathbf{q}_B = 0 \tag{6}$$

The matrix $\mathbf{X}$ in equation (6) is referred to as the sensitivity matrix. The elements of this matrix are the derivatives of the estimated temperatures at the sampling points with respect to the estimated and then evaluated values of the design variable, i.e. the elements of the vector $\mathbf{q}_B$. The matrix $\mathbf{X}$ is defined by

$$\mathbf{X} = \begin{bmatrix} X_{11} & X_{12} & \cdots & X_{1N_q} \\ X_{21} & X_{22} & \cdots & X_{2N_q} \\ \vdots & \vdots & \ddots & \vdots \\ X_{J1} & X_{J2} & \cdots & X_{JN_q} \end{bmatrix} \tag{7}$$

where

$$X_{rs} = \frac{\partial T_r}{\partial q_s} \tag{8}$$

In order to solve equation (6) for the vector $\mathbf{q}_B$, an expression for the vector $\mathbf{T}$ as a function of $\mathbf{q}_B$ should be provided. Such an expression can be obtained by using a few terms of Taylor series expansion of the vector $\mathbf{T}$ in a neighborhood of the vector $\tilde{\mathbf{q}}_B$

$$\mathbf{T}(\mathbf{q}_B) = \tilde{\mathbf{T}} + \mathbf{X}\left(\mathbf{q}_B - \tilde{\mathbf{q}}_B\right) \tag{9}$$

where $\tilde{\mathbf{T}}$ is a vector whose elements are the temperature values at the sampling points when the vector of heat fluxes $\tilde{\mathbf{q}}_B$ is applied on the boundary Γ_q. Substituting equation (9) into equation (6) and after some arithmetic manipulations, the vector $\mathbf{q}_B$ is obtained in the following form

$$\mathbf{q}_B = \left[\mathbf{X}^{\mathrm{T}}\mathbf{X} + \alpha\mathbf{I}\right]^{-1}\left[\mathbf{X}^{T}(\mathbf{Y} - \tilde{\mathbf{T}}) + \mathbf{X}^{\mathrm{T}}\mathbf{X}\tilde{\mathbf{q}}_B\right] \tag{10}$$

Since in this study the thermo-physical properties of the medium are considered to be temperature dependent, the expression obtained for $\mathbf{q}_B$ should be used iteratively until a convergence criterion is satisfied. An equivalent expression for $\mathbf{q}_B$, which is more suitable for iterative calculations, can be written as follows

$$\mathbf{q}_B^{k+1} = \left[\left(\mathbf{X}^k\right)^{\mathrm{T}}\mathbf{X}^k + \alpha^k\mathbf{I}\right]^{-1}\left[\left(\mathbf{X}^k\right)^{\mathrm{T}}(\mathbf{Y} - \mathbf{T}^k) + \left(\mathbf{X}^k\right)^{\mathrm{T}}\mathbf{X}^k\mathbf{q}_B^k\right] \tag{11}$$

where the superscript k refers to the iteration number. In order to use equation (11), the vector of heat fluxes obtained at the preceding time step is used as the initial guess. Also, the temperature-dependent thermophysical properties of the metal are computed based on the temperature distribution at the preceding time step. Equation (11) is repeatedly used until a convergence criterion is fulfilled. In this study, the following criterion is used

$$\|\mathbf{q}_B^{k+1} - \mathbf{q}_B^k\| \leqslant \varepsilon \tag{12}$$

Here, the values of ε in equation (12) are selected according to a desired accuracy.

Selection of the optimal regularization parameter. The appropriate selection of the regularization parameter is of crucial importance when dealing with inverse problems. Low values of the regularization parameter will result in a heat flux vector with a large norm. Generally, this means that the elements of the heat flux vary severely over the boundary Γ_q. On the other hand, large values of α will result in a large difference between the values of the desired and evaluated temperatures at the sampling points. Consequently, there should be a compromise between the loss of accuracy and oscillatory solutions. The L-curve method[33] is a well-known heuristic criterion for the selection of the optimal value for α. Herein, another method is used for the selection of the regularization parameter. In the method presented herein, the optimal value for α is selected such that the difference between the desired and evaluated temperatures at the sampling points would be bounded. More precisely, the following formulation is used

$$e_l \leqslant \mathrm{RMS}\left(\mathbf{T}(\mathbf{q}_B^{k+1}) - \mathbf{Y}\right) \leqslant e_u \tag{13}$$

where e_l and e_u are specified lower and upper bounds, respectively, for the difference between the desired and estimated temperatures. Equation (13) implies that a new value of the regularization parameter is selected at each iteration of the problem analysis. For problems in which a physically feasible pattern for the motion of the solidification front is desired, smaller values of these bounds can be selected. In contrast, for problems in which the desired motion of the solidification front is physically impossible, larger values of these bound should be selected. Based on our numerical experiences, for physically feasible motions, the error bounds can be selected around 0.001–0.005 (0.1–0.5%), while for physically impossible design objectives, the aforementioned bounds should be larger. In such cases, a suitable value of α for which reasonably smooth results are obtained is selected according to the amount by which the desired motion violates the governing equations. In general, the designer might have to select the error bounds based on their engineering judgment and/or a trial and error procedure.

RMS in equation (13) refers to the root mean square function, which for a vector $\mathbf{V}$ of length n is defined as

$$\mathrm{RMS}(\mathbf{V}) = \sqrt{\left(\sum V_i^2\right)/n} \tag{14}$$

By substituting equation (9) into equation (13), the criterion for the selection of the regularization parameter reads as follows

$$e_l \leqslant \mathrm{RMS}\left(\mathbf{T}^k + \mathbf{X}^K(\mathbf{q}_B^{k+1} - \mathbf{q}_B^k) - \mathbf{Y}\right) \leqslant e_u \tag{15}$$

Sensitivity analysis. There are generally two different methods for computing the sensitivity coefficients in equation (8). The first one is based on the direct differentiation of the governing equation with respect to the unknown heat fluxes. In the second method, the finite difference technique is used for the calculation of the derivatives. The former technique is faster, however computationally more complex. In the latter method, which is used in this article, a typical sensitivity element of the matrix $\mathbf{X}$ is obtained according to the following expression

$$X_{rs} = \frac{\partial T_r}{\partial q_s} = \frac{\begin{array}{c} T_r\left(q_1, q_2, \ldots, (1+\delta)q_s, \ldots, q_{N_q}\right) \\ -T_r\left(q_1, q_2, \ldots, q_s, \ldots, q_{N_q}\right) \end{array}}{\delta q_s} \tag{16}$$

where δ is a small number, say 0.01. It should be mentioned that once a reasonably small value for δ is selected, the results are not sensitive to the particular choice of δ because the behavior of the problem will be approximately linear with this small change in the heat flux.

Secondary regularization. At each time step of the inverse problem analysis, the regularization parameter α is used for the reduction of the spatial oscillations in the heat fluxes. However, the heat flux vector may have strong oscillations with respect to time, which makes it difficult to apply the retrieved fluxes in an actual casting process. In this study, a so-called secondary regularization is used to overcome this difficulty, aiming at the reduction of the temporal variations of the calculated heat flux vector.

Suppose that $\mathbf{V}$ is a vector with oscillatory elements. In order to find a vector $\mathbf{V}'$ as close as possible to $\mathbf{V}$, but with non-oscillatory elements, one can minimize the following expression

$$R = \sum_{i=1}^{n} \left(V_i - V_i'\right)^2 + \gamma \sum_{i=2}^{n-1} \left(V_{i+1}' - 2V_i' + V_{i-1}'\right)^2 \tag{17}$$

where n is the number of elements of the vector $\mathbf{V}$ and γ the regularization parameter, whose value can be adjusted to eliminate oscillations as much as required. In general, choosing $\gamma \in [0.5, 5]$ leads to acceptable results. The minimization of R is equivalent to the minimization of expression $|\mathbf{SV}' - \mathbf{K}|$, where

$$S = \begin{bmatrix} \mathbf{I} \\ \gamma \mathbf{H} \end{bmatrix}, \; K = \begin{Bmatrix} \mathbf{V} \\ \mathbf{0} \end{Bmatrix} \tag{18}$$

with $\mathbf{I}$ as the identity matrix and

$$\mathbf{H} = \begin{bmatrix} 0 & 0 & 0 & 0 & 0 \\ 1 & -2 & 1 & 0 & 0 \\ 0 & 1 & -2 & 1 & 0 \\ 0 & 0 & 1 & -2 & 1 \\ 0 & 0 & 0 & 0 & 0 \end{bmatrix} \tag{19}$$

Generally, the matrix $\mathbf{H}$ in equation (19) is an $n \times n$ matrix; however, here this is written for $n = 5$.

The minimization of R with respect to the elements of the vector $\mathbf{V}$ results in the following relation for the vector $\mathbf{V}'$

$$\mathbf{V}' = \left(\mathbf{S}^{\mathrm{T}}\mathbf{S}\right)^{-1}\mathbf{S}^{\mathrm{T}}\mathbf{K} \tag{20}$$

The benefit of the vector expression given in equation (20) for the vector $\mathbf{V}'$ is twofold. First, a vector is obtained with elements that are non-oscillatory. Second, the sums of the elements of vectors $\mathbf{V}$ and $\mathbf{V}'$ are identical.[4] This means that for the problem considered herein, both vectors impose the same amount of energy to the problem domain.

Determination of an appropriate vector of initial guesses. The use of equation (11) for the evaluation of the vector of heat fluxes requires an initial guess for the first iteration, i.e. $\mathbf{q}_B^0$. For the time steps other than the first one, the distribution of heat fluxes obtained in the preceding time step is used as the initial guess. For the first time step, a simple balance of energy can be used for obtaining an initial guess. Since most of the heat extracted from the material in the first time step is due to the latent heat effects, a uniformly distributed heat flux vector which extracts the same amount of energy from the medium can be calculated as an initial guess, i.e.

$$\mathbf{q}_B^0 = \begin{bmatrix} \dfrac{mL}{l_\Gamma \Delta t} & \dfrac{mL}{l_\Gamma \Delta t} & \cdots & \dfrac{mL}{l_\Gamma \Delta t} \end{bmatrix}^{\mathrm{T}} \tag{21}$$

where m is the mass of the metal contained in the first transition zone, L the latent heat of solidification, Δt the time duration of the first time step, and l_Γ the length of the boundary Γ_q. Since the shape of the transition zone is known a priori, the volume and, therefore, the mass of the metal encompassed in each transition zone can be computed without any difficulty.

The meshless RPIM

In the past decade, the rapid development of the processing capabilities of computers resulted in the emergence of new computational techniques with interestingly new abilities. Meshless methods are rather new techniques, built on the idea of reducing or eliminating the need for a predefined mesh during the numerical analysis of problems. These methods have shown great potential for the analysis of problems, for which severe issues occur because of the distortion of the elements or re-meshing processes when analyzed by mesh-based methods. For instance, meshless methods are promising for the numerical analysis of large deformation and metal forming processes,[15] moving and free boundary,[14] and shape optimization problems.[34]

In this study, the meshless RPIM is used for the sensitivity analysis. In addition, to improve the accuracy and efficiency of the RPIM, a meshless integration technique, namely the CTM, is used for evaluating the domain integrals in the formulation of the RPIM. Khosravifard et al.[13] have shown that the IRPIM is well suited for the analysis of non-linear transient problems. Since the sensitivity analysis of this study requires the solution of several non-linear transient heat transfer problems, the meshless IRPIM is utilized for this purpose.

The CTM for meshless evaluation of domain integrals

To improve the capability of the BEM for the treatment of domain integrals, Hematiyan[35,36] proposed an integration technique, namely the CTM. The CTM was originally used for the transformation of domain integrals in the BEM into boundary integrals. The BEM along with the CTM has been efficiently used for the analysis of heat transfer problems[37] as well as thermo-elasticity with non-uniform heat sources.[38] The modified version of the CTM has been successfully applied for the meshless evaluation of domain integrals in mesh-free methods.[13,39] Bui et al.[40] have found the CTM highly appropriate for the evaluation of domain integrals in mesh-free methods.

In the IRPIM, the CTM is applied for the evaluation of domain integrals. In the CTM, the evaluation of a domain integral is performed by the dot product of a vector collecting the values of the integrand at the integration points and a vector containing the CTM integration weights, i.e.

$$I = \int_{\Omega} f(\mathbf{x})\,\mathrm{d}\Omega \cong \sum_{i=1}^{N} W_i^{CTM} f_i = \mathbf{F}^{\mathrm{T}}\mathbf{W}^{CTM} \tag{22}$$

where N is the number of CTM integration points for the domain Ω and W_i^{CTM} the value of the CTM integration weight corresponding to the ith integration point. In equation (22), $f_i = f(\mathbf{x}_i)$ with $\mathbf{x}_i$ the position of the ith integration point. The CTM introduces a systematic procedure for finding the position of the integration points and the associated integration weights without any domain discretization.[39]

Formulation of the IRPIM

In the conventional RPIM, radial and polynomial basis functions are used for the interpolation of a scattered set of data.[41] Suppose that the values of a function $f(\mathbf{x})$ are known at a scattered set of nodes $\mathbf{x}_j, j = 1, 2, \ldots, m$. The RPIM can be used for interpolating this set of data to obtain an approximate value for f at any point of interest $\mathbf{x}$, i.e.

$$f(\mathbf{x}) = \sum_{i=1}^{n} \phi_i(\mathbf{x}) f(\mathbf{x}_i) = \mathbf{\Phi}^{\mathrm{T}}\mathbf{F} \tag{23}$$

where ϕ_i is the shape function of the ith node and n the number of nodes in the support domain of point $\mathbf{x}$. The support domain of any point is a domain in the vicinity of that point which contains the nodes used for the interpolation of data.

In order to obtain a discretized form of the governing equation of solidification, equation (1), the interpolation of equation (23) is used. On using the interpolated form of the temperature function in the associated Galerkin weak-form, a discretized matrix equation of the following form is obtained

$$\mathbf{M}(\mathbf{T})\dot{\mathbf{T}} + \mathbf{K}(\mathbf{T})\mathbf{T} = \mathbf{F} \tag{24}$$

where $\mathbf{T}$ is a vector collecting the nodal values of the temperature within the domain and

$$M_{ij}(\mathbf{T}) = \int_{\Omega} \rho(\mathbf{T}) c(\mathbf{T}) \phi_i \phi_j \,\mathrm{d}\Omega \tag{25}$$

$$K_{ij}(\mathbf{T}) = \int_{\Omega} k(\mathbf{T}) \left[\phi_{i,x}\phi_{j,x} + \phi_{i,y}\phi_{j,y}\right] \mathrm{d}\Omega \tag{26}$$

$$F_i = \int_{\Omega} g(\mathbf{x})\phi_i \,\mathrm{d}\Omega - \int_{\Gamma_q} \bar{q}\phi_i \,\mathrm{d}\Gamma \tag{27}$$

where ϕ_i and ϕ_j are the RPIM shape functions at nodes i and j, respectively. Equation (24) can be solved by using any well-known time marching scheme, such as the Crank–Nicholson method. However, since the thermo-physical properties of the metal are temperature dependent in this study, matrices $\mathbf{K}$ and $\mathbf{M}$ used to obtain the temperature distribution, depend themselves on the temperature distribution. Consequently, an iterative procedure should be utilized to obtain the temperature within the domain.

In the conventional meshless RPIM, the domain integrals in equations (25) to (27) are evaluated with a background mesh. To improve the accuracy and computational efficiency of the meshless method, we use the CTM for the evaluation of these domain integrals. Khosravifard et al.[13] have given detailed expressions for the evaluation of the domain integrals in the IRPIM.

Numerical examples

In this section, the proposed inverse technique is applied to the design of a continuous casting process. Several predefined motions of the solidification front are considered and heat fluxes are obtained accordingly. Finally, the computed heat fluxes are used in a direct analysis by the FEM software package ANSYS and the position of the solidification front based on the evaluated heat flux history is obtained. In this way, the accuracy of the results obtained by the proposed inverse analysis can be assessed.

A continuous casting process is designed, for which the dimension of the section of the casting is $0.30 \times 0.2\,\mathrm{m}^2$. However, as explained in 'Mathematical model of the continuous casting process' section, only a quarter of the section needs to be modeled. Figure 4(a) depicts the problem geometry and boundary conditions. The configuration of the 70 nodes used in the meshless analysis is also shown in Figure 4(b).

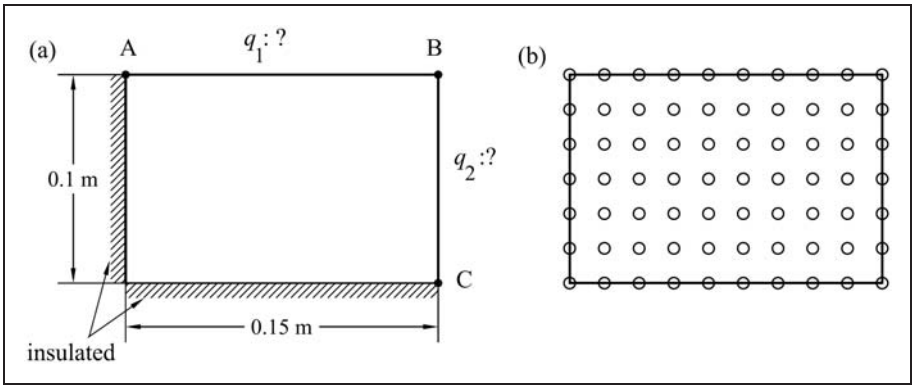

Figure 4. (a) The problem geometry and boundary conditions and (b) nodal arrangement of the IRPIM.

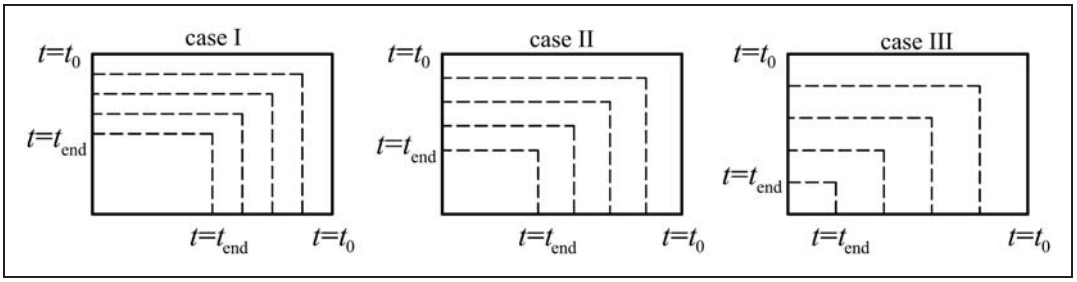

Figure 5. The desired motion of the solidification front.

Table 1. Thermo-physical properties of the casting.

T (K)	300	500	700	900	1100	1300	1500	1700	1809^-	1809^+	1900
c (J/kg·K)	637	672	701	728	753	633	663	825	838	750	750
k (W/m·K)	80	59	48	37	30	30	32	33	35	39	40

The objective of the design is to obtain a heat flux history that would result in a uniform movement of the solidification front parallel to the fixed boundaries of the domain. Three different cases are studied by the examples considered herein. In the first, second, and third cases, the fluxes are obtained such that 75%, 84%, and 96% of the liquid metal are solidified during a specific time interval. The effect of the solidification time on the distribution of heat fluxes is studied in each case. Figure 5 shows the desired motion of the solidification front for each case considered. The dashed lines in this figure represent the desired position of the solidification front at some instances of time.

In each case, for the determination of q_1 and q_2, the upper and right boundaries are divided into six and four segments, respectively. The heat flux at each time step is considered to be constant on each boundary segment. This makes a total of 10 unknown boundary heat fluxes at each time step of the inverse analysis. Also, 20 sampling points are selected at the desired position of the solidification front at each time step. The predefined motion of the solidification front is physically impossible; this is due to sharp corners in the desired shape of the solidification front. However, the inverse technique finds a heat flux history that best matches the desired motion. After obtaining a heat flux history for each case, the secondary regularization is performed to damp the temporal oscillations of the results. The value of the regularization parameter γ, in all cases, is between 0.3 and 1.2.

In all cases considered, calculations are performed for pure iron, for which the melting temperature is 1809 K and the latent heat of solidification is 246 kJ/kg. The pouring temperature is assumed to be 1900 K. The temperature-dependent thermo-physical properties of iron are given in Table 1. The densities of liquid and solid iron used in this article are 7800 and 7900 kg/m^3, respectively.

Case I: 75% of the casting is solidified

In this case, it is desired that 75% of the liquid metal is solidified after a predefined time from the beginning

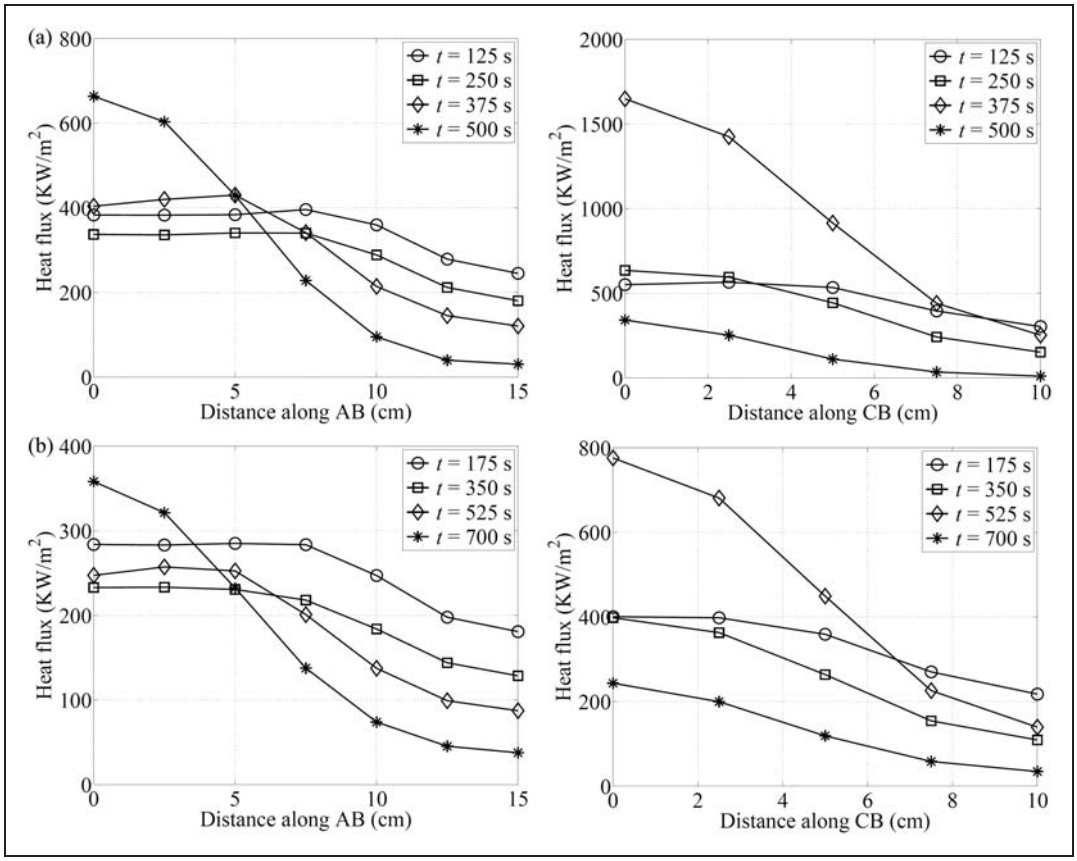

Figure 6. Evaluated heat flux history on the boundary for: (a) $t = 500$ s and (b) $t = 700$ s.

of the casting process. Also, it is required to evaluate a specific history of heat fluxes so that the solidification front would move as depicted in Figure 5. To study the effect of the solidification time on the intensity of the heat fluxes, the inverse analysis is performed for two time durations of 500 and 700 s. Figure 6 plots the heat fluxes q_1 and q_2 for these two time durations of the casting process.

It is observed that by decreasing the solidification time, the intensity of the heat flux vector increases. Therefore, for smaller time durations, the temperature of the solidified material near the boundary Γ_q lowers rapidly. The low temperature of the material near the boundary limits the heat transfer by water sprays. As a result, the solidification time cannot be smaller than a specific value. Otherwise, a heat flux with high intensities would be required, which cannot be attained with water sprays.

Based on the computed values of the heat flux, the position of the solidification front is obtained by ANSYS. The obtained and desired front positions are compared in Figure 7. This figure clearly shows that an acceptable agreement between the desired and obtained front positions exists.

Case II: 84% of the casting is solidified

In this case, it is desired that 84% of the liquid metal be solidified after a predefined time from the beginning of the casting process. In addition, the front motion is desired to be as close as possible to the motion shown in Figure 5. Similar to the previous case, two different time durations of the casting process are chosen and the fluxes are obtained accordingly. Figure 8 plots the evaluated heat fluxes for time durations of 800 and 1000 s, respectively.

The heat flux histories shown in Figure 8 are used in a direct analysis using ANSYS and the solidification front position at some time instances are obtained. The obtained and desired solidification front positions for the time durations of 800 and 1000 s are depicted in Figure 9. A close agreement between the desired and obtained front positions is again observed.

Case III: 96% of the casting is solidified

In the last case, it is desired that 96% of the liquid metal is solidified after a predefined time from the beginning of the casting process. In addition, the front motion is desired to be as close as possible to the motion shown in Figure 5. Two time durations of 1000 and 1200 s are selected for the casting process and the heat fluxes are obtained accordingly. Figure 10 shows the heat flux histories on the boundary Γ_q for the two time durations considered.

Similar to the previous cases investigated, the evaluated heat flux histories are used in a direct analysis

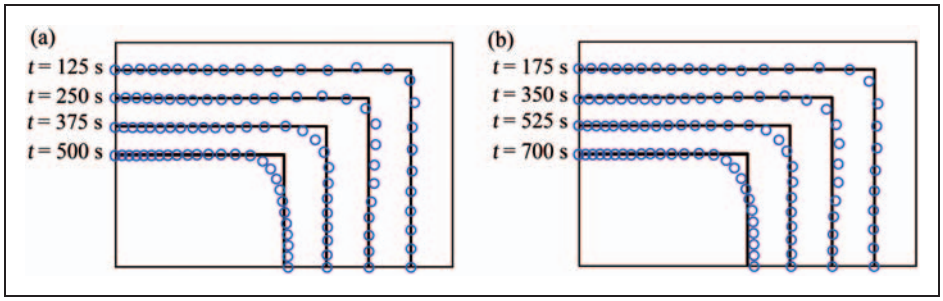

Figure 7. Solidification front position based on the evaluated heat fluxes for: (a) $t = 500$ s and (b) $t = 700$ s.

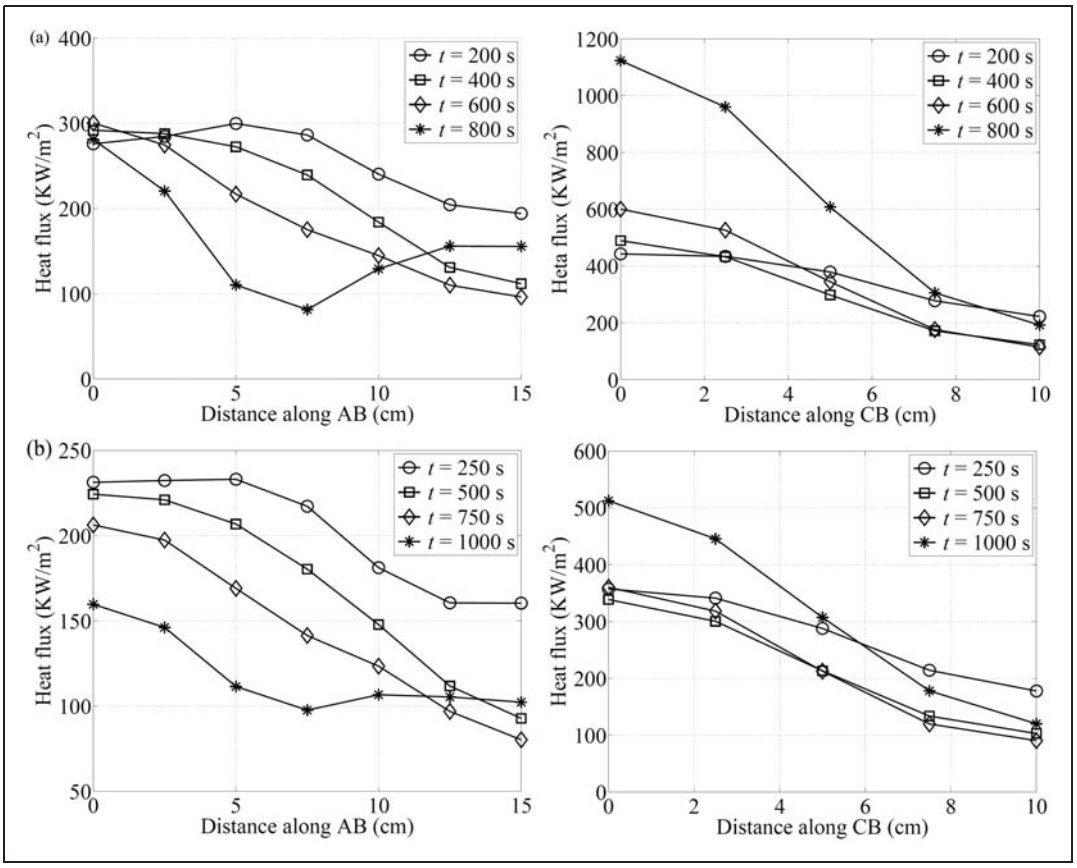

Figure 8. Evaluated heat flux history on the boundary for: (a) $t = 800$ s and (b) $t = 1000$ s.

by ANSYS and the solidification front position is obtained. The actual and desired front positions at some time instances are plotted in Figure 11. Although at the end of the process the solidification front is far away from the boundary Γ_q and therefore the control of the front position becomes difficult, acceptable results are obtained.

To study the effect of the number of time steps of the inverse analysis on the accuracy of the results, the analysis is performed once by regarding four time steps and once by eight time steps. The solidification fronts obtained from the heat fluxes of each case are compared in Figure 12. It can be seen from this figure that increasing the number of time steps improves the accuracy of the actual front position. However, the results obtained by four time steps are still satisfactory.

As explained in 'Secondary regularization' section, a so-called secondary regularization is performed on the vector of heat fluxes in order to damp the temporal oscillations of the results. Figure 13 depicts the heat flux on one segment of the boundary Γ_q, with and without performing the secondary regularization. This figure clearly shows how the secondary regularization employed reduces the oscillations and, consequently, makes the design process more applicable.

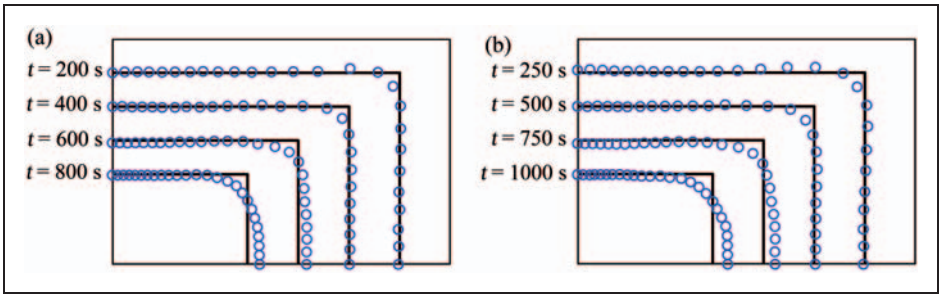

Figure 9. Solidification front position based on the evaluated heat fluxes for: (a) $t = 800$ s and (b) $t = 1000$ s.

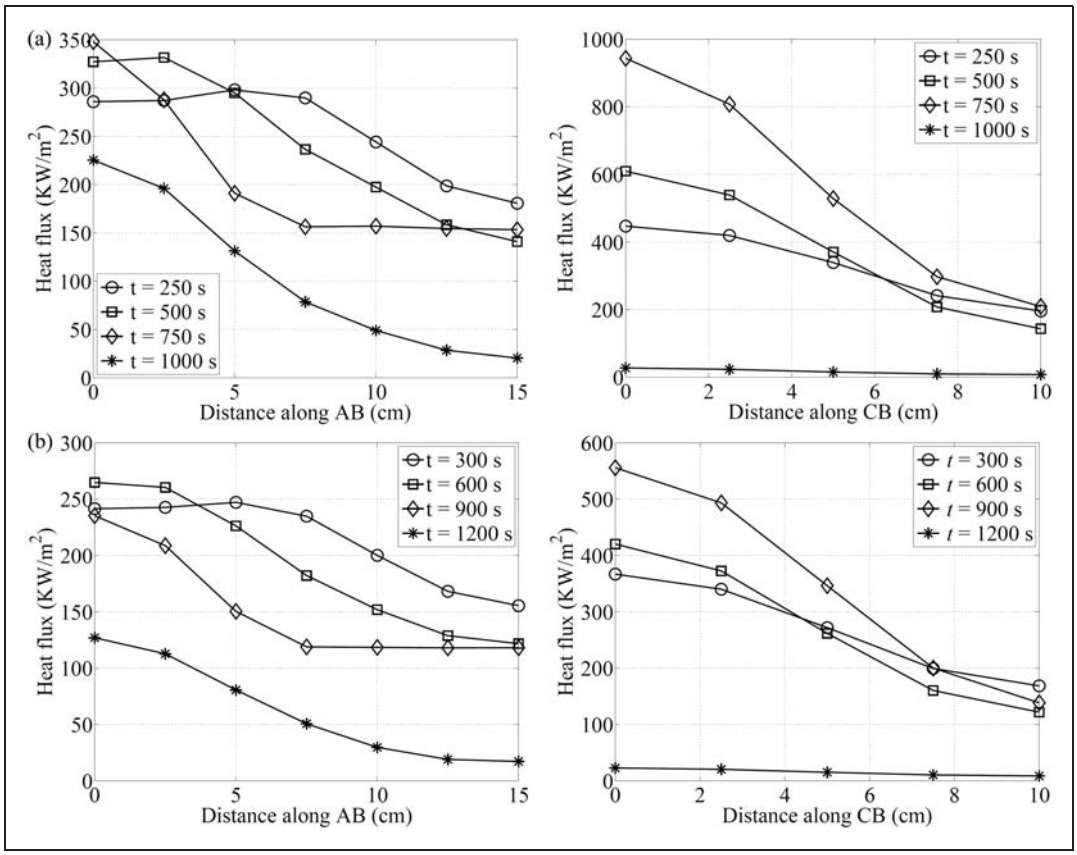

Figure 10. Evaluated heat flux history on the boundary for: (a) $t = 1000$ s and (b) $t = 1200$ s.

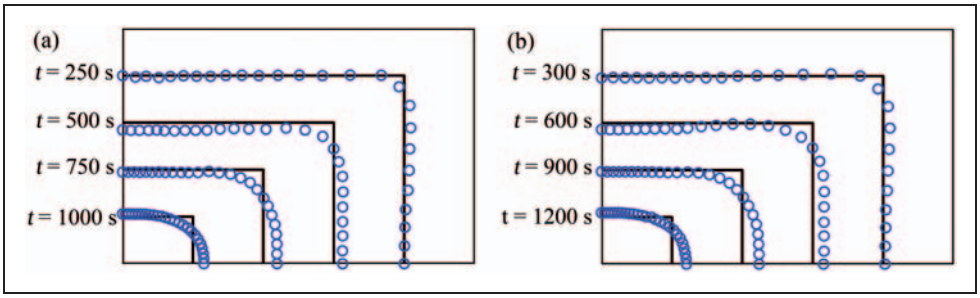

Figure 11. Solidification front position based on the evaluated heat fluxes for: (a) $t = 1000$ s and (b) $t = 1200$ s.

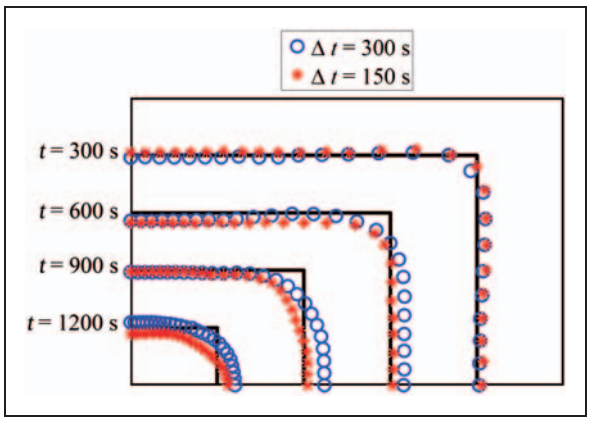

Figure 12. Solidification front position obtained with four and eight time steps.

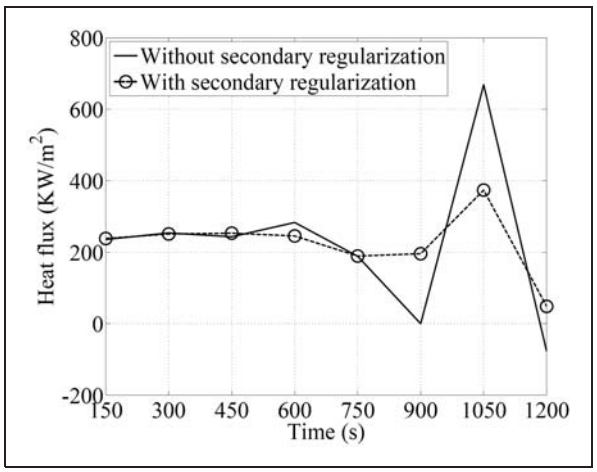

Figure 13. Effect of the secondary regularization on reduction of oscillations in the results.

Conclusions

In this study, a methodology based on an inverse technique for the design of the continuous casting process of pure metals was proposed. This method is based on a pseudo-heat source which accounts for the liberation of the latent heat during the solidification process. By utilizing the pseudo-heat source method, the inverse solidification problem is transformed into an inverse heat conduction problem which can be tackled more efficiently than the original problem. The formulation of the proposed method is made for the case in which all thermo-physical properties of the medium are temperature dependent. Therefore, the method is applicable to the design of actual casting processes that occur over a large temperature interval. In the proposed method, first, a desired motion of the solidification front is selected. Then, by the solution of an optimization problem, specific heat fluxes are obtained that would result in an actual motion of the front that best matches the desired one. As an example, the proposed method was applied for the design of the continuous casting of iron. The results obtained for the examples considered herein demonstrate the great potential of the proposed method for accurate and efficient design of casting processes.

Funding

This research received financial support from the Romanian Ministry of Education, Research and Innovation through IDEI Programme, Exploratory Research Complex Projects, Grant PN II-ID-PCCE-100/2009.

References

1. ASM. *Casting ASM metal handbook*. vol. 15, Metals Park, OH: American Society of Metals, 1998.
2. Nowak I, Smolka J and Nowak AJ. An effective 3-D inverse procedure to retrieve cooling conditions in an aluminium alloy continuous casting problem. *Appl Therm Eng* 2010; 30: 1140–1151.
3. Slota D. Restoring boundary conditions in the solidification of pure metals. *Comput Struct* 2011; 55: 155–176.
4. Khosravifard A and Hematiyan MR. Inverse analysis of solidification problems using the mesh-free radial point interpolation method. *Comput Modell Eng Sci* 2011; 78: 185–208.
5. Weckman DC and Niessen P. A numerical simulation of the D.C. continuous casting process including nucleate boiling heat transfer. *Metall Mater Trans B* 1982; 13: 593–602.
6. Laitinen E and Neittaanmäki P. On numerical simulation of the continuous casting process. *J Eng Math* 1988; 22: 335–354.
7. Lally B, Biegler L and Henein H. Finite difference heat-transfer modeling for continuous casting. *Metall Mater Trans B* 1990; 21: 761–770.
8. Theodorakakos A and Bergeles G. Numerical investigation of the interface in a continuous steel casting mold water model. *Metall Mater Trans B* 1998; 29: 1321–1327.
9. Fic A, Nowak AJ and Bialecki R. Heat transfer analysis of the continuous casting process by the front tracking BEM. *Eng Anal Boundary Elem* 2000; 24: 215–223.
10. Ha MY, Lee HG and Seong SH. Numerical simulation of three-dimensional flow, heat transfer, and solidification of steel in continuous casting mold with electromagnetic brake. *J Mater Process Technol* 2003; 133: 322–339.
11. Risso JM, Huespe AE and Cardona A. Thermal stress evaluation in the steel continuous casting process. *Int J Numer Methods Eng* 2006; 65: 1355–1377.
12. Prax C and Sadat H. A low-order meshless model for multidimensional heat conduction problems. *Appl Math Modell* 2011; 35: 4926–4933.
13. Khosravifard A, Hematiyan MR and Marin L. Nonlinear transient heat conduction analysis of functionally graded materials in the presence of heat sources using an improved meshless radial point interpolation method. *Appl Math Modell* 2011; 35: 4157–4174.
14. Zhang L, Rong YM, Shen HF, et al. Solidification modeling in continuous casting by finite point method. *J Mater Process Technol* 2007; 192–193: 511–517.

15. Cleary PW, Prakash M, Das R, et al. Modelling of metal forging using SPH. *Appl Math Modell* 2012; 36: 3836–3855.
16. Zhang L, Shen HF, Rong YM, et al. Numerical simulation on solidification and thermal stress of continuous casting billet in mold based on meshless methods. *Mater Sci Eng A* 2007; 466: 71–78.
17. Ko EY, Yi KW, Park JK, et al. Numerical modeling and analysis of the thermal behavior of copper molds in continuous casting. *Met Mater Int* 2010; 16: 281–288.
18. Engl HW and Langthaler T. Numerical solution of an inverse problem connected with continuous casting of steel. *Math Methods Oper Res* 1985; 29: B185–B199.
19. Binder A, Engl HW and Vessella S. Some inverse problems for a nonlinear parabolic equation connected with continuous casting of steel: stability estimates and regularization. *Numer Funct Anal Optim* 1990; 11: 643–671.
20. Hill JM and Wu YH. On a nonlinear Stefan problem arising in the continuous casting of steel. *Acta Mech* 1994; 107: 183–198.
21. Grever W, Binder A, Engl HW, et al. Optimal cooling strategies in continuous casting of steel with variable casting speed. *Inverse Prob Eng* 1996; 2: 289–300.
22. Nowak I, Nowak AJ and Wrobel LC. Tracking of phase change front for continuous casting – inverse BEM solution. In: M Tanaka and GS Dulikravich (eds) *Inverse problems in engineering mechanics II*. Oxford: Elsevier, 2000, pp.71–80.
23. Cheung N and Garcia A. The use of a heuristic search technique for the optimization of quality of steel billets produced by continuous casting. *Eng Appl Artificial Intell* 2001; 14: 229–238.
24. Nowak I, Nowak AJ and Wrobel LC. Identification of phase change fronts by Bezier splines and BEM. *Int J Therm Sci* 2002; 41: 492–499.
25. Santos CA, Spim JA and Garcia A. Mathematical modeling and optimization strategies (genetic algorithm and knowledge base) applied to the continuous casting of steel. *Eng Appl Artif Intell* 2003; 16: 511–527.
26. Nowak I, Smolka J and Nowak AJ. A reproduction of boundary conditions in three-dimensional continuous casting problem. *World Acad Sci Eng Technol* 2008; 43: 243–248.
27. Slota D. Identification of the cooling condition in 2-D and 3-D continuous casting processes. *Numer Heat Transfer, Part B* 2009; 55: 155–176.
28. Fazeli H and Mirzaei M. A comparative study of two methods for identifying the solid–liquid interface in a cold storage system. *Proc IMechE, Part C: J Mech Eng Sci* 2011; 225: 917–929.
29. Hematiyan MR and Karami G. A boundary elements pseudo heat source method formulation for inverse analysis of solidification problems. *Comput Mech* 2003; 31: 262–271.
30. Racz D and Bui TQ. Novel adaptive meshfree integration techniques in meshless methods. *Int J Numer Methods Eng* 2012; 90: 1414–1434.
31. Bui TQ, Nguyen MN and Zhang C. A moving Kriging interpolation-based element-free Galerkin method for structural dynamic analysis. *Comput Methods Appl Mech Eng* 2011; 200: 1354–1366.
32. Bui TQ, Khosravifard A, Zhang C, et al. Dynamic analysis of sandwich beams with functionally graded core using a truly meshfree radial point interpolation method. *Eng Struct*. Epub ahead of print 2012, DOI: 10.1016/j.engstruct.2012.03.041.
33. Hansen PC. The L-curve and its use in the numerical treatment of inverse problems. In: P Johnston (ed.) *Computational inverse problems in electrocardiology*. Southampton: WIT Press, 2001, pp.119–142.
34. Bobaru S and Mukherjee S. Meshless approach to shape optimization of linear thermoelastic solids. *Int J Numer Methods Eng* 2002; 53: 765–796.
35. Hematiyan MR. A general method for evaluation of 2D and 3D domain integrals without domain discretization and its application in BEM. *Comput Mech* 2007; 39: 509–520.
36. Hematiyan MR. Exact transformation of a wide variety of domain integrals into boundary integrals in boundary element method. *Commun Numer Methods Eng* 2008; 24: 1497–1521.
37. Mohammadi M, Hematiyan MR and Marin L. Boundary element analysis of nonlinear transient heat conduction problems involving non-homogenous and nonlinear heat sources using time-dependent fundamental solutions. *Eng Anal Boundary Elem* 2010; 34: 655–665.
38. Hematiyan MR, Mohammadi M, Marin L, et al. Boundary element analysis of uncoupled transient thermo-elastic problems with time- and space-dependent heat sources. *Appl Math Comput* 2011; 218: 1862–1882.
39. Khosravifard A and Hematiyan MR. A new method for meshless integration in 2D and 3D Galerkin meshfree methods. *Eng Anal Boundary Elem Method* 2010; 34: 30–40.
40. Bui TQ, Nguyen MN and Zhang C. An efficient meshfree method for vibration analysis of laminated composite plates. *Comput Mech* 2011; 48: 175–193.
41. Liu GR and Gu YT. *An introduction to meshfree methods and their programming*. New York: Springer, 2005, p.74.